Earth Planets Space, **62**, 829–832, 2010

A new aeromagnetic survey of the North Pole and the Arctic Ocean north of Greenland and Ellesmere Island

Jürgen Matzka[1], Thorkild M. Rasmussen[2], Arne V. Olesen[1], Jens Emil Nielsen[1], Rene Forsberg[1], Nils Olsen[1], John Halpenny[3], and Jacob Verhoef[3]

[1]*DTU Space, Juliane Maries Vej 30, 2100 Copenhagen, Denmark*
[2]*GEUS, Ø. Voldgade 10, 1350 Copenhagen, Denmark*
[3]*NRCan, 580 Booth, Ottawa, ON K1A 0E4, Canada*

(Received May 13, 2010; Revised June 25, 2010; Accepted July 1, 2010; Online published December 31, 2010)

We present a preliminary analysis of more than 50,000 km of aeromagnetic survey lines flown in the Arctic Ocean, acquired in 2009 with an optically pumped scalar magnetometer as part of the airborne geophysical survey 'LOMGRAV'. From the observations we removed main and magnetospheric fields as given by the CHAOS-3 field model (Olsen *et al*., 2010) and remaining external fields as monitored by the Canadian magnetic observatory Alert. The reduced data were levelled based on cross-over differences at line intersections. Finally, a grid was computed, upward continued by 3500 m and compared with the EMAG2 grid (Maus *et al*., 2009), showing a good general agreement but also areas with systematic differences. The obtained data are expected to be part of the next version of the World Digital Magnetic Anomaly Map (WDMAM).
Key words: Aeromagnetic survey, Arctic Ocean, WDMAM, Greenland, Ellesmere Island.

1. Introduction

Total magnetic field measurements were taken in the spring of 2009 as part of the airborne geophysical survey 'LOMGRAV', which covers a significant part of the Arctic Ocean. The LOMGRAV survey was a joint Danish-Canadian gravity and magnetic survey, aimed at collecting supporting geophysical data for extended continental claims according to Article 76 in the United Nations Convention on the Law of the Sea (UNCLOS). The LOMGRAV magnetic survey supplements earlier basin-wide magnetic surveys from both US and Russian sources (Glebovsky *et al*., 1998; Brozena *et al*., 2003). The new data are a valuable extension of the data used for global mapping of the geomagnetic field and will be made available for the next generation of the World Digital Magnetic Anomaly Map (WDMAM) as an upward continued grid. For the WDMAM, available near-surface (aeromagnetic or marine magnetic survey) data, e.g. the gridded data compilation for the Arctic by the Geological Survey of Canada (Verhoef *et al*., 1996) have been used for the present version, called WDMAM 2007 (Korhonen *et al*., 2007). However, for parts of the Arctic and other regions of the world where no near-surface data were available, WDMAM 2007 is based on downward-continued satellite data or on crustal age models combined with a polarity time scale (Korhonen *et al*., 2007). Since the release of WDMAM 2007, the Arctic grid compilation CAMP-GM became available (Gaina *et al*., 2008), which was used for the global EMAG-2 grid (Maus *et al*., 2009) and the more recent EMM crustal magnetic anomaly model (Maus, 2010).

The aeromagnetic survey described here covers an area of 550,000 km^2 centred approximately at 87°N, 70°W. It has an irregular boundary along the coast of Ellesmere Island and Greenland and includes the North Pole (Fig. 1(a, b)). More than 50,000 km of survey lines were flown with a Basler DC-3 between March 24 and May 10, 2009, from remote airfields in Canada and Greenland. The flight path was optimised for gravity data collection, and most data were acquired at an altitude of 600 m above sea level, but the radial connector lines from Eureka and Station Nord to the survey lines (Fig. 1(a)) were flown mostly at altitudes between 2000 and 2500 m. The magnetic field measurements were made with a scalar caesium magnetometer (G-823A by *Geometrics*) at the tip of a 6 m long tail boom. The sampling rate was 10 Hz, corresponding to a measurement every 8 m. Additional instruments flown include a fluxgate vector magnetometer (Merayo *et al*., 2009), mounted at 1.5 m distance from the G-823A magnetometer, and two LaCoste & Romberg air/sea gravimeters, S-99 and SL-1. Aircraft attitude was measured with a custom-made Inertial Measurement Unit (IMU). Aircraft position and time stamping for the scalar magnetometer was determined with Javad geodetic grade GPS receivers using the real-time code solution.

2. Preliminary Processing of the Aeromagnetic Data

The positions corresponding to each of the 10 Hz magnetic scalar data points were linearly interpolated from the 1 Hz aircraft positions. For the preliminary processing described here we have not explicitly accounted for the air-

doi:10.5047/eps.2010.07.002

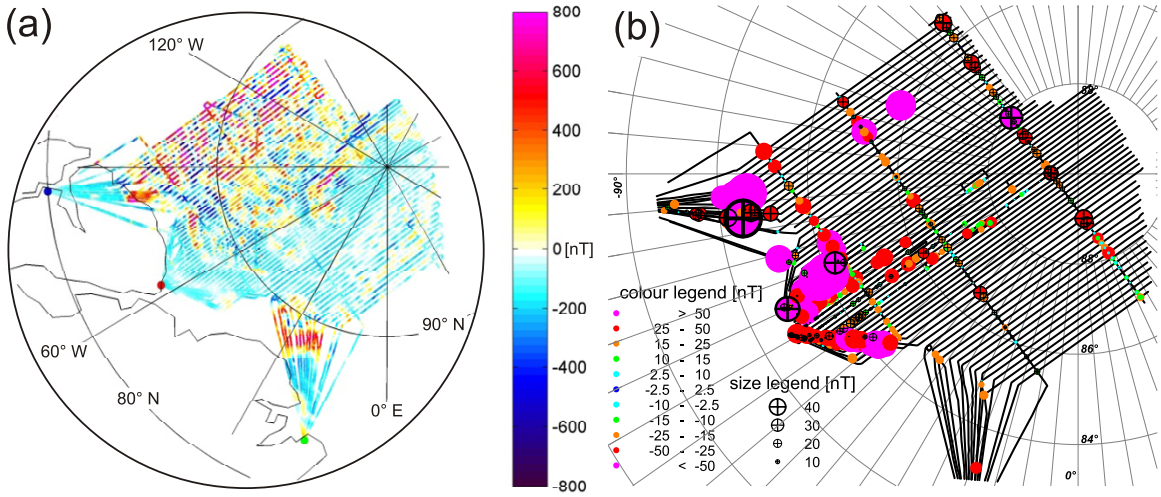

Fig. 1. (a): Map of survey area north of Greenland and Ellesmere Island. The colour code shows field strength ΔF_{survey} in nT after removal of the main field and the external field (see text for details). Eureka and Alert in Canada are marked in blue and red symbols, respectively, while Station Nord in Greenland is marked in green; all three locations have airfields and permanently installed magnetometers. (b): Flight lines and cross-over differences after step three of the line levelling procedure (see text). Cross-over difference absolute values are represented by colours as well as symbol size as shown in the legends; positive values are indicated by a cross and a circle within the symbol, negative values without cross and circle. Cross-over differences occur also within traverse lines, e.g. from 360° turns of the aircraft for the gravity survey.

craft magnetic field. Since its influence on the scalar measurements mainly depends on the orientation of the aircraft with respect to the magnetic field vector (heading error) and the large aircraft followed individual lines very smoothly, we rely on its removal by the applied line levelling technique.

Prior to line levelling, the survey data were reduced as described in the following. For every magnetic scalar field measurement $F_{\text{survey}}(t)$ at location $\mathbf{x}(t)$ we calculate a model field strength $F_{\text{model}}(\mathbf{x}, t) = |\mathbf{B}_{\text{model}}(\mathbf{x}, t)|$. $\mathbf{B}_{\text{model}}$ accounts both for the main field (spherical harmonic degrees $n = 1$ to 15) and for the external and induced magnetospheric field and is calculated from the CHAOS-3 model (Olsen *et al.*, 2010), where the strength of the magnetospheric field is parameterised by the D_{st}-index (more precisely, by its decomposition into E_{st} and I_{st} (Maus and Weidelt, 2004)). To account for the remaining geomagnetic variations in the area, base station data are used. The geomagnetic observatories Eureka and Alert operated by NRCan and the variometer station Station Nord operated by DTU Space are all in the vicinity of the survey area (see Fig. 1(a)), but Alert (IAGA code ALE) is closest to the centre of the survey and linearly interpolated Alert 1-minute total field data $F_{\text{ALE}}(t)$ were used to calculate the reduced survey data $\Delta F_{\text{survey}}(t)$ according to

$$\Delta F_{\text{survey}}(t) = F_{\text{survey}}(\mathbf{x}, t) - F_{\text{model}}(\mathbf{x}, t) - \delta F_{\text{ext}} \qquad (1)$$

with $\delta F_{\text{ext}} = F_{\text{ALE}}(t) - F_{\text{model}}(\mathbf{x}_0, t) - F_{\text{bias}}$ as correction of external field contributions that are not monitored by CHAOS-3. Here $\mathbf{x}_0$ is the location of ALE (82.497°N, 297.647°E) and $F_{\text{bias}} = 57$ nT is the observatory bias of ALE with respect to CHAOS-3, obtained from the requirement that the mean of δF_{ext} over the survey period vanishes. This observatory bias includes for example those crustal field contributions at ALE that are not resolved in the main field model. The resulting reduced survey data $\Delta F_{\text{survey}}(t)$ are shown in Fig. 1(a).

The LOMGRAV survey, like most airborne surveys, includes a large number of parallel, densely spaced traverse lines and a number of tie-lines with larger line spacing flown orthogonal to the traverse lines. During line levelling, differences in data values at intersections of traverse lines with tie-lines (cross-over differences) are taken into account to reduce errors arising from data offsets between adjacent survey lines (e.g. heading errors) or imperfect temporal reduction which could otherwise lead to severe artefacts during gridding (Pilkington and Thurston, 2001).

In the LOMGRAV survey, however, also intersections of traverse lines exist, both in the main survey area and in the radial flight lines from and to the three airfields (Fig. 1(a, b)). Additionally, some flights included sections from more than one traverse line or parts of traverse lines were flown more than once. Occasionally, intersecting or overlapping lines were flown at different altitudes. Furthermore, each of the three prominent tie-lines (North, Centre, South) are broken up into partly overlapping sections. To account for these features, some of the lines with deviating altitude were removed and an adaptive line levelling procedure was performed on the reduced survey data ΔF_{survey}. In this procedure, we distinguish between tie-line cross-over differences and traverse-line cross-over differences. Firstly, the flight lines were split into separate traverse lines and tie-lines. Spacing is about 12 to 15 km for the traverse lines in the main survey area, 316 km between the North tie-line and the Centre tie-line and 240 km between the Centre and the South tie-line (Fig. 1(b)). The North, Centre and South tie-line consists of two, three and four partly overlapping sections, respectively. Secondly, the sections of each tie-line were merged by shifting ΔF_{survey} by a constant offset for each section such that the shifted data mean values are identical in the overlapping parts. The offsets are be-

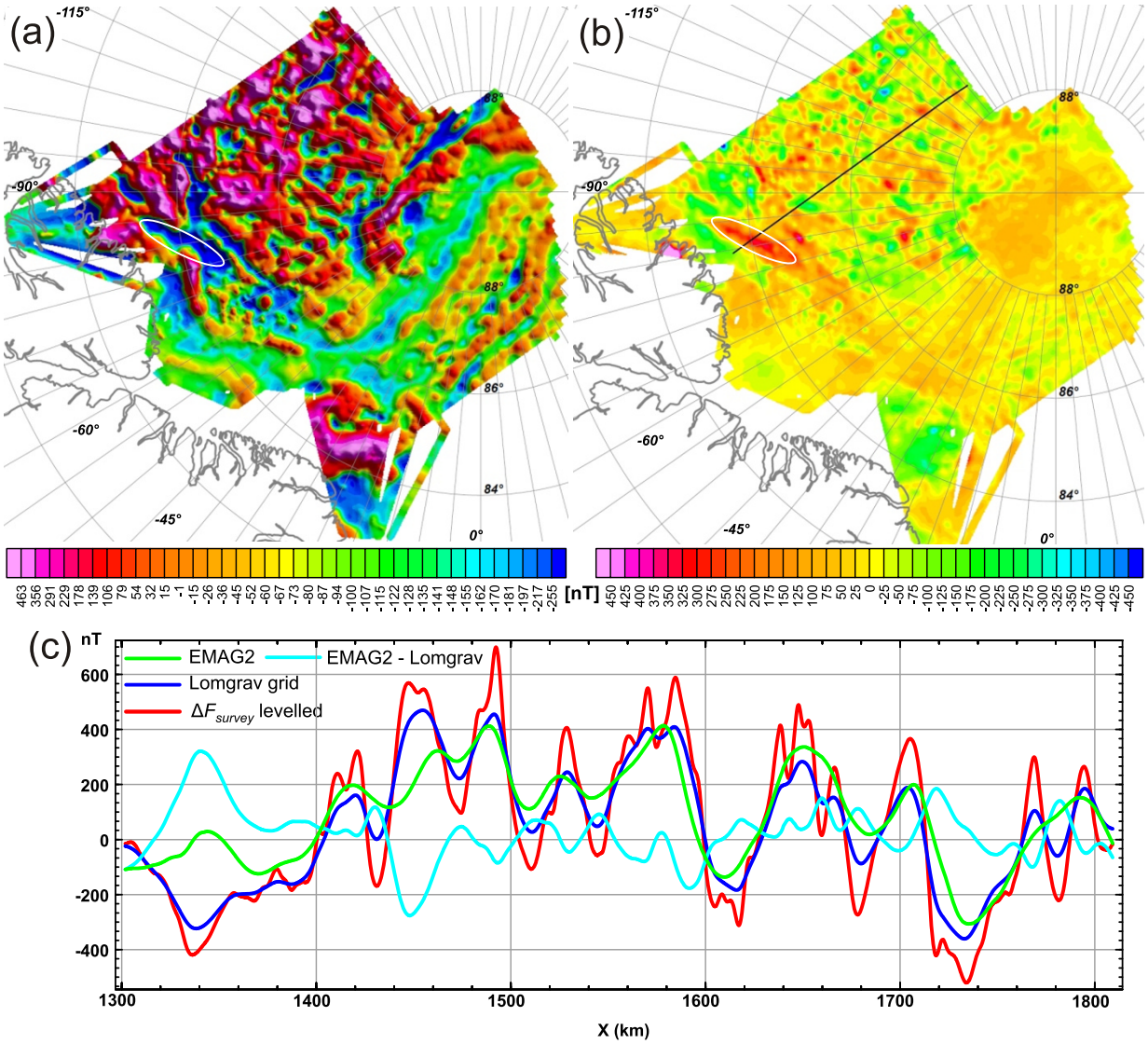

Fig. 2. (a): LOMGRAV magnetic total field anomaly grid upward continued 3500 m above flight altitude, i.e. to an altitude of approximately 4100 m above geoid. (b): Difference (detrended by degree 1 polynomial) of LOMGRAV grid to EMAG2 grid shows generally good agreement between these grids; an area with systematic deviation is marked with a white ellipse in (a) and (b). (c): Levelled survey data as well as grid data along the traverse line indicated as black line in (b).

tween −3.9 nT and −21.1 nT and the mean values are based on about 150 to 1200 measurements, which show a similar variation in the overlapping region. Thirdly, for each merged tie-line, the tie-line cross-over differences were calculated and the tie-line was adjusted by the straight line fit to the cross-over differences. The tie-line cross-over differences after adjustment and the traverse-line cross-over differences are shown in Fig. 1(b). The fourth step is based on the adjusted tie-line cross-over differences. Traverse lines that intersect only two tie-lines were DC-shifted by the mean value of the two tie-line cross-over differences. Traverse lines that intersect three tie-lines were adjusted by a cubic spline function through the three tie-line cross-over differences plus two artificial end points equal to the most adjacent cross-over data, that were added to stabilise the fit. A fifth step is taking into account traverse line cross-over differences from traverse line intersections or repeatedly flown traverse lines, that otherwise pose a problem for gridding, but also give an opportunity to make additional adjustments in the line levelling. This is especially an advantage for the traverse lines that only cross two tie-lines (adjusted by a DC shift in step four). One traverse line after the other was adjusted by a cubic spline similar as in step four, but this time the cubic spline was fitted to both tie-line cross-over differences as well traverse line cross-over differences.

In the LOMGRAV survey some magnetic anomalies have short wavelength compared to the traverse line spacing, leading to artefacts in the interpolated grid data. To avoid these artefacts, we chose to upward continue the gridded data by 3500 m above the flight altitude of approximately 600 m (Fig. 2(a)).

3. Results and Discussion

During the LOMGRAV survey in spring 2009, the external field variations were rather quiet: *Kp* was not exceeding 4, the mean *Kp* was 1 ($Ap = 4.4$). The distance between the base station and the aircraft was up to 800 km and more,

and external field variations of the field strength at Alert were between 20 nT and 120 nT in the course of one day, with typical values around 50 nT. The picture of magnetic anomalies in the reduced data in Fig. 1(a) is coherent and similar to the levelled and gridded data in Fig. 2(a). Also the small offsets between overlapping tie-line sections and the cross-over differences in Fig. 1(b) indicate that the applied reduction is reasonable. However, no quantitative comparison to other possible reduction procedures has been made yet. Despite some complex flight paths, artifacts during gridding are avoided by an adaptive levelling procedure, as can be seen in Fig. 2(a), where the LOMGRAV survey upward continued grid is shown. This final grid can readily be compared to the EMAG2 grid (Maus *et al*., 2009), since both grids are at similar altitude (EMAG2 is at 4000 m, the LOMGRAV grid at about 4100 m) and were reduced using a main field model up to $n = 15$. Subtracting the LOMGRAV grid from the EMAG2 grid and detrending the difference grid by a degree 1 polynomial yields the difference shown in Fig. 2(b). In general, there is a good agreement between EMAG2 and our survey, but systematic deviations occur, e.g. in the area marked by an ellipse at around 84°N, 81°W (Fig. 2(a, b)). Figure 2(c) shows the detrended grid difference (cyan) along a LOMGRAV traverse line (location indicated as black line in Fig. 2(b)) and the survey data ΔF_{survey} after levelling (red). The minimum in the survey data at line position $X \approx 1340$ km confirms that the systematic deviation between the EMAG2 grid and the LOMGRAV grid around 84°N and 81°W (marked by a white ellipse) is not an artefact from gridding. Along the whole traverse line, the LOMGRAV grid (purple in Fig. 2(c)) shows more detail and higher resolution than the EMAG2 grid (green) from the same (or slightly lower) altitude. An obvious example is between $X = 1760$ km and $X = 1800$ km, where the LOMGRAV grid clearly displays two well separated maxima.

The above examples show that the LOMGRAV magnetic grid contains geological information that is not contained in EMAG2, both for larger areas with systematic deviations between the two grids, but also an increased spatial resolution, at least in the direction along its traverse lines. A detailed investigation of this difference, and a possible geological interpretation, is beyond the scope of this note.

Acknowledgments. The LOMGRAV project is financed by the Government of Canada and the Continental Shelf Project of the Kingdom of Denmark. We thank the Polar Continental Shelf Project (NRCan) and the Department of National Defence (Canada) for access to Eureka and Alert and the Defence Command Denmark for access to Station Nord. The geomagnetic observatory at Alert is operated by the Geological Survey of Canada (Natural Resources Canada) and we thank Lorne McKee and David Calp for providing scalar data from Alert. We thank Mark Pilkington and Rick Saltus for their helpful comments on the manuscript.

References

Brozena, J. M., V. A. Childers, L. A. Lawver, L. M. Gahagan, R. Forsberg, J. I. Faleide, and O. Eldholm, New aerogeophysical study of the Eurasia Basin and Lomonosov Ridge: Implications for basin development, *Geology*, **31**(9), 825–828, 2003.

Gaina, C., R. Saltus, C. Harrison, M. St-Onge, A. Alvey, and N. Kusznir, Circum-Arctic Mapping Project: New magnetic anomaly map linked to the geology of the Arctic, in *Eos Trans. AGU*, **89**(53), Fall Meet. Suppl., Abstract GP53B-04, 2008.

Glebovsky, V. Y., L. C. Kovacs, S. P. Mashenkov, and J. M. Brozena, Joint compilation of Russian and US Navy aeromagnetic datain the Central Arctic Seas, *Polarforschung*, **68**, 35–40, 1998.

Korhonen, J. V. *et al*., *Magnetic Anomaly Map of the World (and associated DVD), Scale: 1:50,000,000*, 1st ed., Commission for the Geological Map of the World, Paris, France, 2007.

Maus, S., An ellipsoidal harmonic representation of Earth's lithospheric magnetic field to degree and order 720, *Geochem. Geophys. Geosyst*., **11**, Q06015, doi:10.1029/2010GC003026, 2010.

Maus, S. and P. Weidelt, Separating the magnetospheric disturbance magnetic field into external and transient internal contributions using a 1D conductivity model of the Earth, *Geophys. Res. Lett*., **31**(12), L12,614, 2004.

Maus, S. *et al*., EMAG2: A 2-arc min resolution Earth Magnetic Anomaly Grid compiled from satellite, airborne, and marine magnetic measurements, *Geochem. Geophys. Geosyst*., **10**, Q08005, doi:10.1029/2009GC002471, 2009.

Merayo, J. M. G., T. H. Christensen, P. Brauer, R. Forsberg, F. Primdahl, J. E. Nielsen, and A. V. Olesen, First results from the aeromagnetic survey of the Arctic, in *Abstract book of the IAGA 11th's Scientific Assembly*, 2009.

Olsen, N., M. Mandea, T. J. Sabaka, and L. Tøffner-Clausen, The CHAOS-3 geomagnetic field model and candidates for the 11th generation IGRF, *Earth Planets Space*, **62**, this issue, 719–727, 2010.

Pilkington, M. and J. B. Thurston, Draping corrections for aeromagnetic data: line- versus grid-based approaches, *Expl. Geophys*., **32**, 95–101, 2001.

Verhoef, J., W. R. Roest, R. Macnab, J. Arkani-Hamed, and Project Team, Magnetic anomalies of the Arctic and North Atlantic Oceans and adjacent land areas, *Geological Survey of Canada, Open File 3125a*, 1996.

J. Matzka (e-mail: jrgm@space.dtu.dk), T. M. Rasmussen, A. V. Olesen, J. E. Nielsen, R. Forsberg, N. Olsen, J. Halpenny, and J. Verhoef